

# Approximate probabilistic cellular automata for the dynamics of single-species populations under discrete logistic-like growth with and without weak Allee effects

J. Ricardo G. Mendonça\*

*Escola de Artes, Ciências e Humanidades, Universidade de São Paulo  
Rua Arlindo Bettio 1000, Ermelino Matarazzo, 03828-000 São Paulo, SP, Brazil*

Yeva Gevorgyan†

*Departamento de Matemática Aplicada, Instituto de Matemática e Estatística, Universidade de São Paulo  
Rua do Matão 1010, Cidade Universitária, 05508-090 São Paulo, SP, Brazil*

We investigate one-dimensional elementary probabilistic cellular automata (PCA) whose dynamics in first-order mean field approximation yield discrete logistic-like growth models for a single-species unstructured population with nonoverlapping generations. Beginning with a general six-parameter model, we find constraints on the transition probabilities of the PCA that guarantee that the ensuing approximations make sense in terms of population dynamics and classify the valid combinations thereof. Several possible models display a negative cubic term that can be interpreted as a weak Allee factor. We also investigate the conditions under which a one-parameter PCA derived from the more general six-parameter model can generate valid population growth dynamics. Numerical simulations illustrate the behavior of some of the PCA found. A brief account of the PCA formalism and mean field approximations is included for completeness.

PACS numbers: 87.23.Cc, 05.40.-a, 02.50.-r

Keywords: population dynamics, Allee effect, logistic map, cubic map, cellular automata, mean field approximation

## I. INTRODUCTION

Cellular automata (CA) are discrete-space, discrete-time deterministic dynamical systems that map symbols from a finite set of symbols into the same set of symbols according to some well-defined set of rules. Usually, the discrete dynamical cells that characterize and compose the CA update their states simultaneously, the underlying lattice of cells is regular—like, e.g., an array of equally spaced points or a square or hexagonal lattice—and the dynamics of each cell depends only on the states of other cells over a finite neighborhood. The idea of CA dates back at least to the end of the 1940s, when they were conceived as model systems for simple self-reproducing, self-repairing organisms and, by extension, logical elements and memory storage devices [1]. For broad introductions to the subject see [2–5].

A CA with rules depending on a random variable becomes a probabilistic CA (PCA). PCA were introduced mainly by the Russian school of stochastic processes in the decades of 1960–1970 in relation with the positive probabilities conjecture—a conjecture that is deeply rooted in the theory of Markov processes and has a counterpart in the well-known statistical physics lore that one-dimensional systems do not display phase transitions at finite ( $T > 0$ ) temperature—, but also as model systems for noisy “neurons” and voting systems [6–12]; see also [13, 14]. Besides serving as model systems for the analysis of computation—both applied and theoretical, digital or biological—, CA and PCA (sometimes incarnated as agent-based models) have also been playing a significant role in the modeling of biological and ecological complex systems,

notably spatial processes and the interplay between dispersion and competition in the determination of structure and scale of ecosystems [15–21].

In this paper we investigate how microscopic PCA models of a single-species unstructured population with nonoverlapping generations average in first order, single-cell mean field approximation to well-known models widely employed in population dynamics, namely, the logistic map and a somewhat less well-known variant cubic map that can describe the dynamics of a population under weak Allee effects. The mean field equations provide a connection between the microscopic, local stochastic dynamics of the PCA with the deterministic dynamics of the ensuing discrete-time maps, that otherwise are typically derived using *ad hoc* (phenomenological, at best) arguments that do not necessarily reflect the collective behavior or individual fitness in the population.

The probabilistic nature of the PCA together with the functional form of the logistic and cubic maps that we want to recover from the mean field approximations impose constraints that the microscopic transition probabilities have to observe to make the models sensible from the point of view of population dynamics. Otherwise, the construction of the microscopic PCA models with the desired population dynamics properties from the elementary transitions available is straightforward. We believe that the fact that both the logistic map and a cubic map that incorporates the description of weak Allee effects can be obtained from a single, relatively simple microscopic framework is worth notice. Approaches closely related to ours have been employed in [22, 23]. In particular, in [23] the dynamics of population invasion is modeled as a mixture of birth-death and exclusion processes in discrete space that in the continuum limit becomes a family of reaction-diffusion partial differential equations displaying either Fisher or Allee kinetics with different types of nonlinear diffusivity functions. Their interacting particle systems, however, evolve in contin-

\* Email: jricardo@usp.br

† Email: yeva@ime.usp.br

uous time and are not homogeneous in space. The two approaches are nevertheless close in spirit. A somewhat related approach has also appeared in the sociophysics literature [24].

This paper goes as follows. In Section II we review the logistic growth model in discrete time for the dynamics of a single-species unstructured population with nonoverlapping generations and one of its possible extensions to include Allee effects. Section III presents a reasonably self-contained exposition of the PCA formalism and the mean field approximation to their dynamics. In this section we obtain the first-order, single-cell mean field approximation to the most general one-dimensional left-right symmetric PCA that is central to our analysis and state how we intend to connect it with the discrete maps of population dynamics. In Section IV we derive the constraints on the transition probabilities of the PCA under which its six-parameter mean field approximation yields the logistic map often encountered in population dynamics as well as an extension thereof containing a cubic term that models weak Allee effects. There we also obtain the solution sets in the six-parameter (actually, five-parameter) space that encompass the models of interest, present by way of illustration simulations of some of the valid PCA models obtained, and discuss their main features. Single-parameter PCA are useful as model systems in analytical approaches and also in the study of phase transitions that many PCA display, of several different kinds. Accordingly, in Section V we examine the models that survive the constraints when we reduce the number of parameters of the PCA from six (actually, five) to a single one. We found several, some of which can be understood as probabilistic mixtures of elementary CA. Finally, in Section VI we assess the results obtained, identify loose ends and indicate some research directions that seem to be worth pursuing. An appendix details some calculations in the mean field approximation for some of the single-parameter PCA found.

## II. DISCRETE LOGISTIC-LIKE GROWTH MODELS

### A. The discrete logistic growth model

The dynamics of a single-species population subject to limiting resources can be described by the logistic growth model [25, 26]

$$\frac{dx_t}{dt} = x_t g(x_t) = rx_t \left(1 - \frac{x_t}{K}\right), \quad (1)$$

where  $x_t \geq 0$  represents the size of the population,  $r > 0$  is the maximum potential rate of reproduction of the individuals in the population, and  $K > 0$  is the carrying capacity, defined as the maximum population viable under the given ecological conditions. One can rescale the variables in (1) by  $t \rightarrow rt$  and  $x_t \rightarrow Kx_t$ , but this is not relevant for our discussion. The function  $g(x_t)$  represents the intrinsic growth rate per capita of the population, and the form of the right-hand side of (1) guarantees that when  $x_t = 0$  there is no spontaneous generation of living organisms. The logistic growth model describes populations with an intrinsic growth rate  $g(x_t) = r(1 - x_t/K)$  that decreases to zero as the population grows large, and arose as

an improvement over the simple model of exponential growth to make it more realistic. Equation (1) can be readily integrated and give rise to a sigmoid curve that saturates ( $t \rightarrow \infty$ ) at  $K$ , with an inflection point at  $t = \ln(K/x_0 - 1)/r$ . The basic model (1) has been generalized in several different ways to account for particular conditions and factors affecting specific populations [27].

Discrete-time models are particularly suited to describe the dynamics of populations with nonoverlapping generations, in which the population growth takes place at discrete intervals of time [28, 29]. This is typically the case for populations of annual plants or insects. The discrete-time version of (1), a. k. a. the logistic map, is given by

$$x_{t+1} = rx_t \left(1 - \frac{x_t}{K}\right). \quad (2)$$

Equation (2) is sometimes presented in the form  $x_{t+1} - x_t = rx_t(1 - x_t/K)$ , which is perhaps biologically more revealing; the two forms, however, are equivalent by the redefinitions  $r \leftrightarrow (1 + r)$  and  $K \leftrightarrow (1 + 1/r)K$ . In discrete-time, the only rescaling possible is  $x_t \rightarrow Kx_t$ . The logistic map (2) displays much more complex a behaviour than (1), having become the archetypal example of chaotic dynamical system [28–33].

In this work we are interested in the logistic map both in its basic form (2) and with an extra term included to take into account Allee effects, that we introduce in the next subsection.

### B. Allee effects

The Allee effect, first discussed in the 1930's, describes a positive correlation between the rate of growth and the density of a population, namely, that at low population densities reproduction and survival of individuals may decline [34–37]. The effect saturates or disappears as populations grow larger. The Allee effect challenges the classical tenet of population dynamics according to which individual fitness is higher at low densities because of lower intraspecific competition. Allee effects can be related with components of individual fitness (the component Allee effect) or with overall mean individual fitness (the demographic Allee effect), that is what in general can be measured in the field. The two effects, component and demographic, are clearly related, although not always in any obvious way. Empirical evidence suggests that Allee effects are caused mainly by mate limitation, debilitated cooperative defense, unsubstantial predator satiation, lack of cooperative feeding, dispersal, and habitat alteration [38, 39]. Recently, it has been argued that tumour growth displays many features of population dynamics, including Allee effects [40].

It is possible to model the demographic Allee effect in several different ways, following different biological rationales [41]. Mathematically, the Allee effect requires that the intrinsic population growth rate function  $g(x_t)$  have a maximum at intermediate densities and decay at low densities. It is also desirable that  $g(x_t)$  decays at high densities from its maximum to display the “logistic effect.” The simplest way to obtain this combined behavior is by multiplying the right-hand side

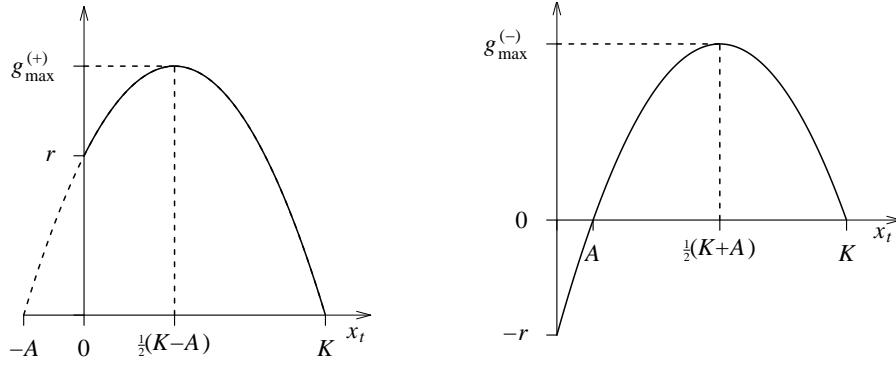


FIG. 1. Intrinsic population growth rate functions  $g^{(+)}(x_t)$  (left panel) and  $g^{(-)}(x_t)$  (right panel) given by (3). The functions have maximum at  $x_{\max}^{(\pm)} = \frac{1}{2}(K \mp A)$ , at which  $g^{(\pm)}(x_{\max}^{(\pm)}) = r(K \pm A)^2/4KA$ . These intrinsic growth rate functions provide models for the weak ( $g^{(+)}(x_t)$ ) and strong ( $g^{(-)}(x_t)$ ) Allee effects.

of (1) or (2) by  $(x_t/A \pm 1)$ , where  $A$  represents a critical population threshold parameter [42–45]. The resulting growth rate function becomes

$$g^{(\pm)}(x_t) = r \left( 1 - \frac{x_t}{K} \right) \left( \frac{x_t}{A} \pm 1 \right), \quad (3)$$

with  $r$ ,  $K$ , and  $A < K$  positive constants. Functions (3) are concave down parabolas with roots located at  $K$  and  $A$  or  $-A$ , to wit,  $g^{(\pm)}(K) = g^{(\pm)}(\mp A) = 0$ , and maximum at  $x_{\max}^{(\pm)} = \frac{1}{2}(K \mp A)$ , where  $g^{(\pm)}(x_{\max}^{(\pm)}) = r(K \pm A)^2/4KA > 0$ . Note that  $g^{(\pm)}(x_{\max}^{(\pm)})$  is always larger than  $g^{(\pm)}(0) = \pm r$ . These functions are depicted in Fig. 1.

Functions  $g^{(\pm)}(x_t)$  model what are known as the weak (or non-critical) Allee effect ( $g^{(+)}(x_t)$ ), according to which at small population sizes the growth rate decreases but remains positive, and the strong (or critical) Allee effect ( $g^{(-)}(x_t)$ ), when the growth rate may become negative at small population sizes and lead the population to extinction. Indeed, from the graph of  $g^{(-)}(x_t)$  in Fig. 1 we see that a population with size greater than  $A$  grows to the carrying capacity  $K$ , while a population that shrinks below the critical threshold  $A$  starts to face negative growth rates that eventually lead it to extinction.

The growth rate functions  $g^{(\pm)}(x_t)$  have been used before in the literature (in the continuous-time setting) to illustrate the dynamics of populations under the influence of Allee effects [42–45]. In this work we only consider models for the weak Allee effect. This is necessary since in the PCA scenario the constant term of the intrinsic population growth rate function becomes a sum of nonnegative probabilities, therefore enforcing the  $g^{(+)}(x_t)$  model, see Sec. IV.

### III. PROBABILISTIC CELLULAR AUTOMATA

#### A. The one-dimensional elementary PCA

The most general one-dimensional elementary PCA [2, 4] is defined by an array of cells arranged in a one-dimensional lattice  $\Lambda = \{1, 2, \dots, L\} \subset \mathbb{Z}$  of total length  $L$ , each cell in one

of the two possible states  $x_i = 0$  or  $1$ ,  $i \in \Lambda$ . Usually the array is made periodic by identifying  $x_{L+1}$  with  $x_1$  and  $x_0$  with  $x_L$ , i. e.,  $\Lambda$  has the topology of a ring (a. k. a. periodic boundary condition). The state of the PCA at integer times  $t = 0, 1, 2, \dots$  is thus given by  $\mathbf{x}^t = (x_1^t, x_2^t, \dots, x_L^t) \in \Omega_\Lambda = \{0, 1\}^\Lambda$ .

The dynamics of the PCA is defined by a transition function  $\Phi : \Omega_\Lambda \rightarrow \Omega_\Lambda$  that given the state  $\mathbf{x}^t$  of the PCA at instant  $t$  determines the state  $\mathbf{x}^{t+1} = \Phi(\mathbf{x}^t)$  of the PCA at instant  $t + 1$ . The transition function is composed by local rules that map the state of each cell  $x_i^t$  into a new state  $x_i^{t+1}$  depending only on a finite neighborhood of  $i$ . In one-dimensional elementary CA and PCA, the neighborhood consists of the cell  $i$  itself together with its left and right nearest neighbors cells  $i \pm 1$ . For PCA, the local transition functions are, in fact, conditional transition probabilities  $\phi(x_i^{t+1} | x_{i-1}^t, x_i^t, x_{i+1}^t)$ , that represent the probability at which the transition  $x_i^t \rightarrow x_i^{t+1}$  occurs in one time step given the current neighborhood of  $x_i^t$  (see Subsec. III B). For systems homogeneous in space and time, these transition functions do not depend on the particular cell  $i$  or time  $t$ , and we write them simply as  $\phi(x_i^t | x_{i-1}, x_i, x_{i+1})$ , where we have kept the index  $i$  just to better identify the neighborhood. Clearly,

$$\sum_{x_i^t} \phi(x_i^t | x_{i-1}, x_i, x_{i+1}) = 1, \quad (4)$$

which is a simple restatement of the fact that the probabilities of all possible transitions  $x_i \rightarrow x_i'$  must add to 1. For elementary PCA,  $x_i = 0$  or  $1$  and we have

$$\phi(0 | x_{i-1}, x_i, x_{i+1}) = 1 - \phi(1 | x_{i-1}, x_i, x_{i+1}), \quad (5)$$

such that we need to specify only, say, the eight possible transitions  $\phi(1 | x_{i-1}, x_i, x_{i+1})$ . A logical choice for most models of natural phenomena are left-right symmetric rules, in which case the transition probabilities further observe

$$\phi(x_i' | x_{i-1}, x_i, x_{i+1}) = \phi(x_i' | x_{i+1}, x_i, x_{i-1}) \quad (6)$$

and we are left with six transition probabilities to specify. We will denote these transition probabilities by  $a, b, \dots, f \in [0, 1]$

TABLE I. Rule table for the general left-right symmetric one-dimensional elementary PCA. The first row lists the initial neighborhood and the other two rows give the probability at which the central cell reaches the state given in the leftmost column; cf. (7a)–(7f).

	111	110	101	100	011	010	001	000
0	$1-f$	$1-d$	$1-e$	$1-b$	$1-d$	$1-c$	$1-b$	$1-a$
1	$f$	$d$	$e$	$b$	$d$	$c$	$b$	$a$

according to the following convention:

$$\phi(1|000) = a, \quad (7a)$$

$$\phi(1|001) = \phi(1|100) = b, \quad (7b)$$

$$\phi(1|010) = c, \quad (7c)$$

$$\phi(1|011) = \phi(1|110) = d, \quad (7d)$$

$$\phi(1|101) = e, \quad (7e)$$

$$\phi(1|111) = f. \quad (7f)$$

These six numbers constitute the free parameters of the model. The rules for a CA or PCA are also usually represented as a table; Table I displays the rule table for PCA (7a)–(7f). Whatever one wants to model with a left-right symmetric elementary one-dimensional PCA must be encoded in the choice of these parameters. We want to model single-species populations under logistic growth with such PCA. If we identify a cell in the state 0 as an empty site or patch and a cell in the state 1 as an individual, the interpretation of the probabilities (7) in terms of population dynamics is immediate. For example,  $a$  represents the probability of spontaneous generation,  $000 \rightarrow 010$ , a somewhat unnatural biological process (see Subsec. IV A), while  $b$  represents the probability of reproduction leading from local configurations 001 or 100 to, respectively, 011 or 110. In the same way,  $f$  represents the

probability of survival of the central individual ( $111 \rightarrow 111$ ) in a possibly overcrowded neighborhood. Not every set of values for the parameters yield sensible models from a population dynamics point of view, though. Further contextual interpretations of these parameters are discussed in Subsec. IV B.

## B. The stochastic dynamics of the PCA

Since the dynamics of PCA is stochastic, given the current state of the PCA we cannot tell for sure what will be its state in the next instant. All that we can detail is what will be the probability  $P_{t+1}(\mathbf{x})$  of observing a particular state  $\mathbf{x}$  in the next instant of time as a weighted sum of contributions from the possible current states, where, for simplicity, we have passed the index  $t$  from the state  $\mathbf{x}$  to the probability mass function, as usual. The probability of observing a particular state at any given time thus obeys

$$P_{t+1}(\mathbf{x}') = \sum_{\mathbf{x}} \Phi(\mathbf{x}'|\mathbf{x}) P_t(\mathbf{x}), \quad (8)$$

where the summation runs over all  $\mathbf{x} \in \Omega_\Lambda$  and  $\Phi(\mathbf{x}'|\mathbf{x}) \geq 0$  is the conditional probability for the transition  $\mathbf{x} \rightarrow \mathbf{x}'$  to occur in one time step. Since the cells of the PCA are updated simultaneously and independently we have

$$\Phi(\mathbf{x}'|\mathbf{x}) = \prod_{i=1}^L \phi(x'_i|x_{i-1}, x_i, x_{i+1}). \quad (9)$$

We can write down the equation for the marginal probability distribution  $P_t(x_k, x_{k+1}, \dots, x_l)$  of observing a block of  $l - k + 1$  consecutive cells in state  $(x_k, x_{k+1}, \dots, x_l)$  by summing  $P_t(\mathbf{x})$  over the variables  $x_1, \dots, x_{k-1}, x_{l+1}, \dots, x_L$ . From equations (4), (8), and (9), the dynamics of such marginal probability distributions is given by

$$P_{t+1}(x'_k, x'_{k+1}, \dots, x'_l) = \sum_{x_{k-1}, x_k, \dots, x_{l+1}} \left[ \prod_{i=k}^l \phi(x'_i|x_{i-1}, x_i, x_{i+1}) \right] P_t(x_{k-1}, x_k, \dots, x_{l+1}), \quad (10)$$

and we see that the probability of observing  $l - k + 1$  consecutive cells in a given state at instant  $t + 1$  depends on the probabilities of observing the state of  $l - k + 3$  cells at instant  $t$ . The problem thus constitutes a many-body problem that can be fully solved only very rarely. In order to gain some insight on the dynamics of the PCA we must therefore, in general, resort either to approximate solutions or to numerical simulations. In what follows we describe the mean field approximation that we are going to employ to find relevant PCA that can model single-species populations under logistic growth regimes.

## C. Mean field approximations for the PCA dynamics

The most basic information about the state of the PCA is provided by  $P_t(x)$ , the probability of observing a cell—any cell, since the PCA is homogeneous—in state  $x$  at instant  $t$ . Clearly,  $P_t(x)$  also represents the instantaneous density of cells in state  $x$  in the PCA. According to (10), the dynamics of  $P_t(x)$  is given by

$$P_{t+1}(x'_i) = \sum_{x_{i-1}, x_i, x_{i+1}} \phi(x'_i|x_{i-1}, x_i, x_{i+1}) P_t(x_{i-1}, x_i, x_{i+1}), \quad (11)$$

which leads, as we have already mentioned, to the problem of calculating  $P_t(x_{i-1}, x_i, x_{i+1})$ , which in turn would lead to the problem of calculating  $P_t(x_{i-2}, x_{i-1}, x_i, x_{i+1}, x_{i+2})$  and so on.



In order to solve (11), we must somehow break the hierarchy of coupled equations implied by (10) to get a closed set of equations. The simplest strategy consists in taking the approximation

$$P_t(x_{i-1}, x_i, x_{i+1}) \approx P_t(x_{i-1})P_t(x_i)P_t(x_{i+1}), \quad (12)$$

which embodies the assumption of independence between the cells. Higher order approximations try, by the same token, to approximate correlations of a given order by correlations of lower orders by the generalized scheme

$$P_t(x_k, x_{k+1}, \dots, x_l) \approx \frac{P(x_k, \dots, x_{l-1})P(x_{k+1}, \dots, x_l)}{P(x_{k+1}, \dots, x_{l-1})}. \quad (13)$$

These so-called cluster (or Bayesian) approximations were developed for CA and PCA in [46, 47]; see also [48–51]. The application of mean field approximations of higher orders requires considerable tinkering to find suitable combinations of variables that simplify the nonlinear equations that follow, and it is not uncommon to employ computer algebra systems in the task.

In this work we investigate the one-dimensional PCA defined by the transition probabilities (7) in the single-cell, first order mean field approximation given by (12). As we will see, already at this level of approximation we obtain several interesting models of single-species population dynamics.

#### D. The first order, single-cell mean field approximation

Let us obtain the mean field equations that are going to be the focus of our attention for the rest of this paper. Equation (11) for  $P_t(x'_i = 1) = P_t(1)$ , in the elementary PCA defined by the left-right symmetric transition probabilities (7) reads

$$\begin{aligned} P_{t+1}(1) = & aP_t(0, 0, 0) + b[P_t(0, 0, 1) + P_t(1, 0, 0)] \\ & + cP_t(0, 1, 0) + d[P_t(0, 1, 1) + P_t(1, 1, 0)] \\ & + eP_t(1, 0, 1) + fP_t(1, 1, 1). \end{aligned} \quad (14)$$

Applying the single-cell mean field approximation (12) to the probabilities that appear on the right-hand side of (14) and writing  $P_t(1) = x_t$ ,  $P_t(0) = 1 - x_t$  we obtain

$$\begin{aligned} x_{t+1} = & a(1 - x_t)^3 + (2b + c)x_t(1 - x_t)^2 \\ & + (2d + e)x_t^2(1 - x_t) + fx_t^3. \end{aligned} \quad (15)$$

In the next section we determine the conditions on the transition probabilities  $a, b, \dots, f$  that can turn (15) into one of the population growth models (2) or (3).

### IV. PCA MODELS OF LOGISTIC POPULATION GROWTH

#### A. Constraints on the transition probabilities

Although the set of transition probabilities (7) are the most general possible for an elementary one-dimensional left-right

symmetric PCA, when  $\phi(1|000) = a \neq 0$  there are spontaneous generation of living organisms, an undesirable feature for biological population models. To make model (15) biologically sensible, thus, we must require that  $a = 0$ . This is our first constraint on the transition probabilities if we want to obtain valid population growth models. When we set  $a = 0$ , equation (15) becomes  $x_{t+1} = x_t h(x_t)$ , with  $h(x_t)$  given by

$$\begin{aligned} h(x_t) = & (2b + c) + [(2d + e) - 2(2b + c)]x_t \\ & + [(2b + c) - (2d + e) + f]x_t^2. \end{aligned} \quad (16)$$

Now notice that the transition probabilities  $b$  and  $c$  always appear in (15) and (16) in the combination  $2b + c$ . This happens because in the mean field approximation (12) to (14),  $P_t(0, 0, 1)$ ,  $P_t(0, 1, 0)$ , and  $P_t(1, 0, 0)$ , that are respectively associated with the transition probabilities  $\phi(1|001) = b$ ,  $\phi(1|010) = c$ , and  $\phi(1|100) = b$ , all give rise to the same term  $x_t(1 - x_t)^2$ ; i.e., in the single-cell mean field approximation, only the number of individuals in the initial neighborhood matters for the dynamics. *Ditto* for the transition probabilities  $d$  and  $e$ , that always appear together like  $2d + e$ . It is thus convenient to lump these transition probabilities into new variables  $u = 2b + c$  and  $v = 2d + e$ , both in the range  $0 \leq u, v \leq 3$ .

Comparing the mean field equation (16) for the dynamics of the PCA (7) with models (2) and (3) for the growth of a single-species population, we see that the coefficients of the powers of  $x_t$  in (16), that we will denote by  $[1]$ ,  $[x_t]$  and  $[x_t^2]$ , must obey, in terms of the new variables  $u$  and  $v$ , one of the two following sets of constraints:

**Case I (Logistic map):** To recover (2) from (16) we must have  $[x_t^2] = 0$  together with  $[1] > 0$  and  $[x_t] < 0$ . These constraints translate into the following conditions on the transition probabilities of the PCA:

$$u > 0, \quad (17a)$$

$$-2u + v < 0, \quad (17b)$$

$$u - v + f = 0. \quad (17c)$$

**Case II (Cubic map with weak Allee effect):** In this case, to recover the  $g^{(+)}(x_t)$  model in (3) from (16),  $[x_t^2]$  must be negative while both  $[1]$  and  $[x_t]$  must be positive. In terms of the transition probabilities these conditions read

$$u > 0, \quad (18a)$$

$$-2u + v > 0, \quad (18b)$$

$$u - v + f < 0. \quad (18c)$$

Note that because  $2b + c \geq 0$  in (16) must be compared with the independent term of  $g^{(\pm)}(x_t)$  in (3), the PCA is not able to reproduce  $g^{(+)}(x_t)$ , for which  $g^{(+)}(0) = -r < 0$ , at least not in the single-cell, first order mean field approximation. Otherwise, if  $2b + c = 0$ , i.e., if  $b = c = 0$ ,  $h(x_t)$  in (16) becomes

$$h(x_t) = (2d + e)x_t(1 - x_t). \quad (19)$$

This form for  $h(x_t)$  corresponds to the limit  $A \rightarrow 0$  in (3). Indeed, when  $x_t/A \gg 1$ , we can take  $x_t/A \pm 1 \approx x_t/A$  and obtain

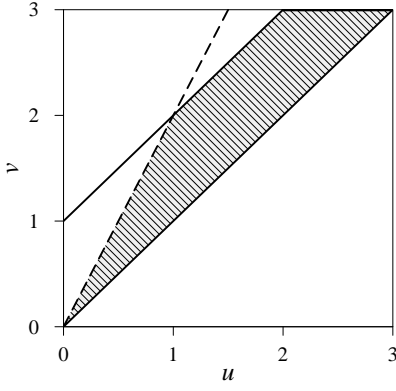


FIG. 2. Projection on the  $uv$ -plane of the solution set  $S_I$  of (20) (hatched area). Given  $(u, v) \in S_I$ ,  $f$  is given by the plane  $f = v - u$  “hovering” over the hatched area. The hatched polygon has vertices at  $(u, v) = (0, 0)$ ,  $(1, 2)$ ,  $(2, 3)$ , and  $(3, 3)$ , with total area  $2/9$ . The dashed edge  $(0, 0) - (1, 2)$  as well as the lines external to the hatched area do not belong to  $S_I$ .

$g^{(\pm)}(x_t) \approx (r/A)x_t(1 - x_t/K)$ , as in (19). The resulting dynamical system then develops a double root at  $x_t = 0$ . The limit  $A \rightarrow 0$  models a particular case of weak Allee effect, since the intrinsic growth rate function never becomes negative in this limit. In this paper, however, we gloss over this limiting case and always take  $A > 0$ .

### B. Analysis of the constraints and some examples

In what follows, most of the times when we mention a transition probability  $b, c, \dots, f$ , we side it with the microscopic transition that it models to facilitate its interpretation.

One can argue that from the point of view of population dynamics the more interesting PCA models are those with small values of  $e$  ( $101 \rightarrow 111$ ) and  $f$  ( $111 \rightarrow 111$ ), to model the decrease of the birth rates in overcrowded neighborhoods (the “logistic effect”), and moderate to large values of  $b$  ( $001 \rightarrow 011$  and  $100 \rightarrow 110$ ) and  $d$  ( $011 \rightarrow 011$  and  $110 \rightarrow 110$ ), to model reproduction and survival under favorable conditions. The magnitude of  $c$  ( $010 \rightarrow 010$ ) depends on whether one wants to model individuals more or less resilient to loneliness and its consequences. Possible choices for the transition probabilities encompassing these arguments would be, for example,  $e = f = b/2$  and  $c = d$  or  $d/2$ , among others. In this subsection we analyse the two sets of constraints identified in Subsec. IV A and give examples of PCA that fall into each case. As we shall see, the classification of PCA into Case I or Case II makes a lot of sense, since the analysis of their transition probabilities can be naturally interpreted as describing the dynamics of a population either under logistic growth or Allee effect regimes.

**Case I (Logistic map):** Constraints (17) can be recast as

$$v < 2u, \quad 0 < u \leq v \leq 1 + u, \quad (20)$$

with  $f = v - u$  always in the range  $[0, 1]$ . Problem (20) is effectively a two-dimensional problem. Fig. 2 displays the pro-

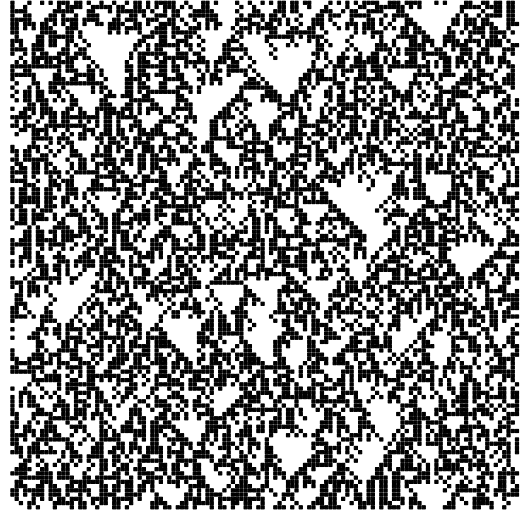


FIG. 3. Space-time diagram of PCA  $(a, b, c, d, e, f) = (0, \frac{2}{3}, \frac{1}{3}, \frac{7}{8}, \frac{1}{4}, \frac{1}{3})$  exemplifying Case I. A total of 120 cells under periodic boundary conditions are evolved for 120 time steps (time runs downwards) from an initially random state of density  $1/2$ .

jection  $\{v < 2u\} \cap \{0 < u \leq v \leq 1 + u\}$  of the solution set  $S_I$  on the  $uv$ -plane. The solution set  $S_I$  includes the plane  $f = v - u$ , that however is not displayed in Fig. 2. The  $uv$ -projection of  $S_I$  occupies a considerable fraction (namely,  $2/9$ ) of the  $[0, 3] \times [0, 3]$  box available. That means that it is not hard to find a set of transition probabilities satisfying (20) that also makes sense in terms of population dynamics. For example, we can take  $b = 2/3$  ( $001 \rightarrow 011$  and  $100 \rightarrow 110$ ) to represent relatively high, but not certain, reproduction in a relatively favorable neighborhood,  $c = 1/3$  ( $010 \rightarrow 010$ ) and  $d = 7/8$  ( $011 \rightarrow 011$  and  $110 \rightarrow 110$ ) to represent survival, with  $c$  smaller than  $d$  (or, even more significantly, smaller than  $d/2$ ) because of the “loneliness factor,” and  $e = 1/4$  ( $101 \rightarrow 111$ ) again to represent possible but not certain (in fact, unlikely) reproduction into a crowded neighborhood. We then obtain  $u = 2b + c = 5/3$ ,  $v = 2d + e = 2$ , and  $f = v - u = 1/3$  ( $111 \rightarrow 111$ ) representing the possibility of survival in what we may call an overcrowded neighborhood. A space-time diagram of the resulting PCA is displayed in Fig. 3 for a PCA of length  $L = 120$  initially occupied by  $L/2 = 60$  individuals randomly distributed among the cells.

The equivalent logistic map (2) for the above choice of transition probabilities has  $r = u = 5/3$ , within the interval of stability [28–33], and  $K = u/(2u - v) = 5/4$ , namely,

$$x_{t+1} = \frac{5}{3}x_t \left(1 - \frac{4}{5}x_t\right). \quad (21)$$

The stationary density of the logistic map (21) is given by  $x_\infty = 1/2$ , while the average stationary density of the PCA measured from small scale simulations is  $\langle x_\infty^{(\text{PCA})} \rangle \simeq 0.484$ . Not bad for a single-cell mean field approximation.

**Case II (Cubic map with weak Allee effect):** Constraints (18) are equivalent to

$$0 < 2u < v, \quad f < v - u. \quad (22)$$

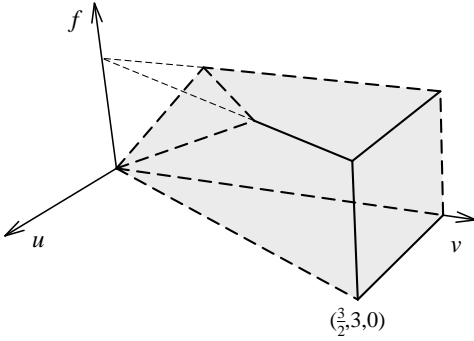


FIG. 4. Solution set  $S_{II}$  (shaded volume) of (22). The simplex has vertices at  $(u, v, f) = (0, 0, 0)$ ,  $(\frac{3}{2}, 3, 0)$ ,  $(0, 3, 0)$  (lower face),  $(1, 2, 1)$ ,  $(\frac{3}{2}, 3, 1)$ ,  $(0, 3, 1)$ ,  $(0, 1, 1)$  (upper face), with total volume  $|S_{II}| = 25/12$ . Dashed edges as well as faces bounded by dashed edges do not belong to  $S_{II}$ .

The solution set  $S_{II}$  of (22) can be constructed as follows. In a coordinate system  $(u, v, f)$ , the first constraint  $0 < 2u < v$  determines a triangular slab delimited by the planes  $u = 0$ ,  $v = 3$  and  $v = 2u$  contained in the box  $(0, 3] \times (0, 3] \times [0, 1]$ . The second constraint defines a half-space bounded above by the plane  $f = v - u$ , i. e., by a plane normal to the direction  $(1, -1, 1)$ . The intersection of this half-space with the triangular slab is  $S_{II}$ . This set is depicted in Fig. 4. Note that the triangle with vertices at  $(0, 0)$ ,  $(0, 1)$  and  $(1, 2)$  in Fig. 2 is but the projection of the tilted triangular face of  $S_{II}$  onto the  $uv$ -plane. Clearly, since  $[x_i]$  must be either positive or negative, the two solution sets are disjoint,  $S_I \cap S_{II} = \emptyset$ .

The volume of  $S_{II}$  is  $25/12$ , approximately 23% of the total volume available, so that there is plenty of valid sets of transition probabilities to choose from. In this case, however, choices with large values of  $b$  ( $001 \rightarrow 011$  and  $100 \rightarrow 110$ ), that we argued formerly represent populations better prepared to thrive, are less numerous, since  $u < 3/2$  in  $S_{II}$ , entailing  $b < 3/4$ , that moreover can be large only at the expense of  $c$  ( $010 \rightarrow 010$ ), that then has to be small. In other words, for a given valid  $u$ , if we pick  $b > 1/2$  we necessarily have to pick  $c < 1/2$  and vice-versa; we cannot have both probabilities above  $1/2$  as in Case I. For instance, if we pick  $b = 2/3$ , as in the previous example, we have to pick  $c < 1/6$ , meaning that, on average, less than one out of six lone individuals ( $010$ ) survive to tell the history. This is a manifestation of the Allee effect, seen from the point of view of the local microscopic processes. Another manifestation of the Allee effect in the opposite direction is reflected on the possible choices for  $v$ , that can be as large as the maximum possible, namely,  $v = 3$ . Large values of  $v$  means large values of  $d$  ( $011 \rightarrow 011$  and  $110 \rightarrow 110$ ) and  $e$  ( $101 \rightarrow 111$ ), that can be interpreted as improved survival probability due to collective support despite the logistic (overcrowding) effect. Whatever the value of  $v$ , the transition probabilities  $b$  ( $001 \rightarrow 011$  and  $100 \rightarrow 110$ ) and  $c$  ( $010 \rightarrow 010$ ) are bound by the condition  $u < v/2$ , further limiting the chances of “unassisted” reproduction ( $b$ ) and survival of lone individuals ( $c$ ). Figure 5 depicts the space-time diagram of a Case II PCA of length  $L = 120$  with pa-

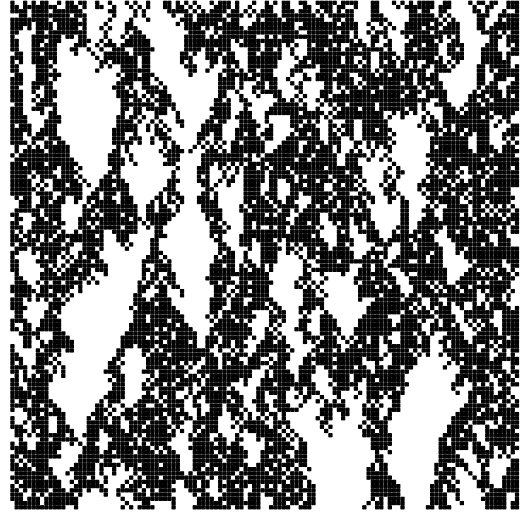


FIG. 5. Space-time diagram of PCA  $(a, b, c, d, e, f) = (0, \frac{3}{8}, \frac{2}{5}, \frac{4}{5}, \frac{3}{4}, \frac{4}{5})$  exemplifying Case II. A total of 120 cells under periodic boundary conditions are evolved for 120 time steps (time runs downwards) from an initially random state of density  $1/2$ .

rameters  $(a, b, c, d, e, f) = (0, \frac{3}{8}, \frac{2}{5}, \frac{4}{5}, \frac{3}{4}, \frac{4}{5})$  initially occupied by  $L/2 = 60$  individuals at random cells.

Note how the clusters of individuals in Fig. 5 are more compact than the clusters in Fig. 3. Also note how some of the clusters are fringed by checkerboard-like regions of low populational density before the plains devoid of individuals. This kind of pattern is typical of invasion processes, in which Allee effects play a major role [22, 23, 42–44]. Invasion processes, however, are better modeled in two spatial dimensions.

The pattern displayed by the PCA in Fig. 5 strongly resembles the pattern of directed (site or bond) percolation clusters at or slightly above criticality [18, 48, 49]. The relationship of these PCA (both Case I and II) with site, bond, and compact percolation processes as well as with other known CA and PCA, in particular with the Domany-Kinzel (DK) PCA [52], is an interesting and not very difficult question. One thing that we can tell in advance is that the map to the DK PCA would require that  $c = 0$ ; exact correspondence would additionally require that  $b = d$  and  $e = f$ . A PCA with the same parameters as the one in Fig. 5 but with  $c = 0$  would roughly correspond to an inactive instance of the DK PCA. It thus seems that sustained activity of the PCA in Case II depends to a certain extent on the survival probability of lone individuals, as embodied by the transition probability  $c = \phi(1|010)$ . Preliminary analysis suggests that the dynamics of the PCA is not very sensitive to the particular values of  $c$  as long as  $c > 0$ .

## V. SINGLE-PARAMETER PCA

Most PCA models in the literature are one and two-parameter models, since they are already rich and flexible enough to model a great many phenomena, in one or more dimensions, and display a variety of nontrivial behavior, from

disordered and chaotic phases to phase transitions of several different kinds [2–5, 48–51]. Two well-known representatives of such PCA are Toom’s north-east-center voting model [10], that helped to foster a whole research program on the foundations of statistical mechanics and theoretical computer science, and the Domany-Kinzel PCA, that holds connections with Ising models, percolation, self-organized criticality, and other encompassing ideas [52]. It is thus not entirely without interest to identify single-parameter PCA that in the single-cell mean field approximation yield models for the logistic growth of populations, with or without Allee effects.

#### A. Parametrization of the transition probabilities

We can reduce the number of parameters of PCA (7) from six to a single one, say,  $p \in \mathbb{R}$ , by parametrizing the transition probabilities like  $a(p), b(p), \dots, f(p) : \mathbb{R} \rightarrow [0, 1]$ . This parametrization has advantages and disadvantages. The main advantage is simplicity, since it is practically hopeless to try to calibrate six parameters of such a simple PCA model, all of the same order of magnitude, with field data without incurring into serious risk of overfitting. The simplification also helps in the exploratory study, analytical or numerical, of the models. A big disadvantage is the drastic reduction in the number of models, since now the set of transition probabilities traces a one-dimensional curve (however convoluted) of zero measure in an otherwise much larger six-dimensional manifold.

The simplest possible parametrization of the transition probabilities is by linear functions,  $a(p) = a_0 + a_1 p$ ,  $b(p) = b_0 + b_1 p$ ,  $\dots$ ,  $f(p) = f_0 + f_1 p$ , with  $p \in [p_1, p_2]$ . Each function will then be of the form  $(p - p_1)/(p_2 - p_1)$  (increasing from 0 to 1) or  $(p_2 - p)/(p_2 - p_1)$  (decreasing from 1 to 0). Common choices for  $[p_1, p_2]$  are  $[-1, 1]$  and  $[0, 1]$ . We do not have reasons to choose any one particular interval for  $p$ , so we choose  $p \in [0, 1]$  and the transition probabilities become then given either by  $p$  or  $q = 1 - p$ . In this case, we end up with  $2^6 = 64$  possible parametrizations for the transition probabilities, namely,  $(a, b, c, d, e, f) = (p, p, p, p, p, p)$ ,  $(p, p, p, p, p, q)$ ,  $\dots$ ,  $(q, q, q, q, q, q)$ . Now, note that since  $q = 1 - p \Leftrightarrow p = 1 - q$ , if a given parametrization has solution set  $p \in (p_1, p_2]$  (we take a half-open, half-closed interval for the sake of illustration), interchanging the roles of  $p$  and  $q$  in the parametrization leads to the “dual” parametrization with solution set  $q \in (p_1, p_2]$ , that is,  $p \in [1 - p_2, 1 - p_1]$ . As a consequence, as  $p$  ranges over the interval  $[1 - p_2, 1 - p_1]$ , the transition probabilities of the dual parametrization range over the same values as the given parametrization when  $p$  ranges over  $(p_1, p_2]$ , and the two parametrizations are equal. We then see that only a maximum of 32 parametrizations are unique because of this symmetry.

In our study, as before and for the same reasons (see Subsec. IV A), we set  $a(p) = 0$ . In this way we have to examine only 16 possible parametrizations of the transition probabilities. Again, it is convenient to look at these parametrizations through the variables  $u = 2b + c$  and  $v = 2d + e$ . Within these settings, we now determine for which values of  $p$  PCA (7) comply with constraints (17) and (18).

TABLE II. Solution sets for the one-parameter version of PCA in Case I (logistic map) according to the possible parametrizations indicated in the first column. The solution sets are given as line segments (equations in symmetric form) in the  $(u, v, f)$  space. In every case  $f = (2d + e) - (2b + c) = v - u$ .

$(a, b, c, d, e, f)$	$S_I(a, b, c, d, e, f; p)$
$(0, p, p, p, p, *)$	$u/3 = v/3 \in (0, 1], f = 0$
$(0, p, p, p, q, *)$	$u/3 = v - 1 = (1 - f)/2 \in (\frac{1}{3}, \frac{1}{2}]$
$(0, p, p, q, p, *)$	$u/3 = 2 - v = (2 - f)/4 \in (\frac{2}{7}, \frac{1}{2}]$
$(0, p, p, q, q, *)$	$u/3 = (3 - v)/3 = (3 - f)/6 \in (\frac{1}{3}, \frac{1}{2}]$
$(0, p, q, p, p, *)$	$u - 1 = v/3 = (1 + f)/2 \in [\frac{1}{2}, 1]$
$(0, p, q, p, q, *)$	$u - 1 = v - 1 \in [0, 1], f = 0$
$(0, p, q, q, p, *)$	$u - 1 = 2 - v = (1 - f)/2 \in (0, \frac{1}{2}]$
$(0, p, q, q, q, *)$	$u - 1 = (3 - v)/3 = (2 - f)/4 \in [\frac{1}{4}, \frac{1}{2}]$

**Case I (Logistic map):** In this case  $f = (2d + e) - (2b + c) = f(b(p), c(p), d(p), e(p))$ , and we have to examine only the 8 possible parametrizations for  $b, c, d$ , and  $e$ . We then enforce constraints (17) on the parametrized transition probabilities and obtain the valid ranges for  $p$  in each case. The solution sets  $S_I(a, b, c, d, e, f; p)$  found are summarized in Table II. Let us look at one example closely to make Table II more clear. If we take  $(a, b, c, d) = (p, p, q, p)$ , we have  $u = 2b + c = 3p$  and  $v = 2d + e = 2 - p$ . The constraint  $u > 0$  (17a) implies  $p > 0$ , while the constraint  $2u > v$  (17b) implies  $p > 2/7$ . Since  $f = v - u = 2 - 4p$  must be a number between 0 and 1, we further require that  $1/4 \leq p \leq 1/2$ . The final solution set is the interval  $p \in (2/7, 1/2]$ . Solutions can also be read as line segments in  $S_I$ . In our example, the equation for the line segment in symmetric form is  $u/3 = 2 - v = (2 - f)/4 = p$ , with  $p \in (2/7, 1/2]$ .

On a side note, we remark that when we take the dual of a given parametrization for a PCA in Case I we observe  $f \leftrightarrow -f$ . This can be seen by rewriting  $f = 2(d - b) + (e - c)$ ; then, for whatever parametrization we have for  $b, c, d$ , and  $e$ , interchanging  $p \leftrightarrow 1 - p$  takes  $f$  into  $-f$ . As  $f > 0$  when  $p \in (p_1, p_2]$ , it follows that  $-f > 0$  as  $p \in (1 - p_2, 1 - p_1]$ ; see the example above.

**Case II (Cubic map with weak Allee effect):** Here we have all 5 transition probabilities  $b, c, d, e$  and  $f$  to parametrize, and we have to scrutinize 16 different parametrizations to get the whole picture. However, from constraint (18c) (or Fig. 4) we see that all instances with  $u = v$  are forbidden, ruling out the 4 parametrizations  $(0, p, p, p, p, *)$  and  $(0, p, q, p, q, *)$ . Other 4 parametrizations violate constraint (18b), namely,  $(0, p, q, p, p, *)$  and  $(0, p, q, q, p, *)$ , because the first ones require that  $p > 2$  and the second ones that  $p < 0$ . At the end we are left with only 8 possible parametrizations to examine. Upon examination, we found that parametrization  $(0, p, p, p, q, q)$  is also impossible because it would also require that  $p < 0$ . The resulting nonempty solution sets are listed in Table III.



TABLE III. Solution sets for the one-parameter version of PCA in Case II (cubic map with weak Allee effect) according to the possible parametrizations indicated in the first column. The solution sets are given as line segments (equations in symmetric form) in the  $(u, v, f)$  space. The last column gives the mixed rule specification of the PCA.

$(a, b, c, d, e, f)$	$S_{II}(a, b, c, d, e, f; p)$	Mixed PCA rule
$(0, p, p, p, q, p)$	$u/3 = v - 1 = f \in (0, \frac{1}{5})$	$p222-q32$
$(0, p, p, q, p, p)$	$u/3 = 2 - v = f \in (0, \frac{2}{7})$	$p182-q72$
$(0, p, p, q, p, q)$	$u/3 = 2 - v = 1 - f \in (0, \frac{2}{7})$	$p54-q200$
$(0, p, p, q, q, p)$	$u/3 = (3 - v)/3 = f \in (0, \frac{1}{3})$	$p150-q104$
$(0, p, p, q, q, q)$	$u/3 = (3 - v)/3 = 1 - f \in (0, \frac{1}{3})$	$p22-q232$
$(0, p, q, q, q, p)$	$u - 1 = (3 - v)/3 = f \in [0, \frac{1}{3})$	$p146-q108$
$(0, p, q, q, q, q)$	$u - 1 = (3 - v)/3 = 1 - f \in [0, \frac{1}{3})$	$p18-q236$

### B. Mixed CA and PCA

The one-parameter PCA in Case II are examples of mixed PCA that have appeared in the literature before [51, 53, 54]. In a mixed PCA, two or more deterministic CA rules are combined probabilistically such that sometimes one rule is applied, sometimes another rule is applied to a given cell. Mixed PCA are closely related with asynchronous PCA [51]. In an asynchronous PCA, one of the rules is the identity map  $x_i^{t+1} = x_i^t$ . Such PCA are also known as “diluted,” their composite rule corresponding to a dilution of the respective non-trivial part. We can specify mixed PCA by telling which rules are applied with which probabilities. For example, the rule table for PCA  $(a, b, c, d, e, f) = (0, p, p, q, p, q)$ , third line in Table III, appears in Table IV. This table corresponds to a transposed arrangement of the usual rule table for CA and PCA (see, e.g., Table I). Reading the lines of the table as binary numbers (Wolfram’s encoding scheme [2]) we obtain that PCA  $(0, p, p, q, p, q)$  is the mixed PCA  $p54-q200$ . In [53], the authors studied the closely related mixed PCA  $p182-q200$ . The two models differ in the probability  $f$  for the transition  $111 \rightarrow 111$ , that is  $\phi(1|111) = p$  in PCA  $p54-q200$  and  $\phi(1|111) = 1$  in PCA  $p182-q200$ . This single difference, however, implies that PCA  $p182-q200$  has two absorbing configurations, the all-0 (empty lattice) and the all-1 (full lattice) configurations. PCA  $p182-q200$  displays an extinction-survival phase transition at the critical point  $p = p^* \simeq 0.488$  in the directed percolation universality class of critical behaviour. PCA  $p54-q200$  also has an extinction-survival phase transition between the empty lattice and a stationary state with finite positive density at  $p^* \simeq 0.575$ , out of the interval  $p \in (0, \frac{1}{7})$  in which the PCA yields (in the mean field approximation) a valid logistic growth model with weak Allee effect. Mean field as well as numerical estimates of the critical points for the mixed PCA of Table III are given in the appendix.

Most likely, models within the same class (I or II) possess similar dynamical behavior and share common features like the distribution of cluster sizes and others. However, given the rich dynamical diversity of the logistic and cubic maps, it would be interesting to explore the PCA found in this section more closely. We defer this investigation to the future.

TABLE IV. Rule table for PCA  $(a, b, c, d, e, f) = (0, p, p, q, p, q)$ , third line in Table III. The first row lists the initial neighborhood and the other two rows give the state that the central cell reaches with the probability given in the first column. This is mixed PCA  $p54-q200$ .

	111	110	101	100	011	010	001	000
$p$	0	0	1	1	0	1	1	0
$q$	1	1	0	0	1	0	0	0

## VI. SUMMARY AND CONCLUSIONS

We explored the modeling possibilities of the most general right-left symmetric one-dimensional elementary PCA to the dynamics of a single-species unstructured population with nonoverlapping generations. Our results consist in the classification of all sets of parameters of the PCA that furnishes in first-order mean field approximation either the logistic map for the density of a population or a cubic map that describes the dynamics of a population under weak Allee effects. The PCA found are composed of microscopic transitions that model the expected behavior or fitness of individuals in a most natural manner. The PCA that give rise to the logistic map, for example, are composed of microscopic transitions that describe individuals that struggle against overcrowded neighborhoods, that hamper their chances of reproducing and survival (small probabilities for transitions like  $101 \rightarrow 111$  and  $111 \rightarrow 111$ ) and prefer more capacious environments (large probabilities for transitions like  $010 \rightarrow 010$  and  $100 \rightarrow 110$ ). In the same manner, the PCA that furnish the cubic map for the dynamics of a population under weak Allee effects is made of microscopic transitions that describe individuals that prefer to team up as long as the neighborhood is not too crowded (relatively high probabilities for events like  $011 \rightarrow 011$  and  $101 \rightarrow 111$ ) but suffer from loneliness (smaller chances that  $001 \rightarrow 011$  and  $010 \rightarrow 010$ ). A detailed analysis and interpretation of two examples was given in Sec. IV B.

We found (somewhat reversely) that the rationale embodied in the choice of the microscopic processes and transition probabilities that enter the PCA model not only provides a satisfactory modeling framework—that has the additional merit of taking into account stochastic fluctuations that, while certainly present in the dynamics of real populations, are otherwise difficult to treat or include in deterministic models—but also provides averaged, mean field equations that describe the dynamics of populations with the expected collective attributes. This is arguably one of our interesting findings.

In Section V we obtained all one-parameter PCA that yield the logistic map for the dynamics of a population density  $x_t$  in the mean field approximation, both in the absence (Case I) and in the presence (Case II) of weak Allee effects. We found 8 different PCA in the first case and 7 in the second case. The PCA in Case II can be viewed as probabilistic mixtures of two different CA rules. All of them display phase transitions between an inactive ( $x_\infty = 0$ ) and an active ( $x_\infty > 0$ ) phase, however at critical points out of the range in which the PCA yield valid models (in the single-cell mean field approximation) for

logistic growth with weak Allee effects. It would be interesting to further investigate the phase transitions in these models irrespective of their connection with the logistic or cubic maps of this work, as well as their relationship with percolation processes and other known CA and PCA.

The analysis of the dynamics of the discrete maps found in this paper was left aside for two reasons. First, because the logistic map (2) is one of the most well studied dynamical systems ever, and we do not feel compelled to add anything to the extensive body of literature concerning its behavior [28–33]. Second, because the dynamics of the full cubic map (15) and its interpretation in the context of population dynamics and Allee effects deserves a detailed investigation that we intend to carry out elsewhere. Although cubic maps have appeared in mathematical biology before [57–59], it seems to be the first time that they are obtained in population dynamics from microscopic models involving the behavior of individual agents.

Clearly, ecological complexity, even at the limited scale of a single-species unstructured population within a single patch, cannot be grasped by a one-dimensional PCA model. One-dimensional CA and PCA models, although aesthetically appealing, are hard to calibrate or verify experimentally. They have, however, the merit of being simple enough to allow for analytical approaches, at least to some degree. Moreover, the PCA transition probabilities can be readily interpreted in population dynamics terms, as we did in Sec. IV (and specially in Sec. IV B). One obvious extension of our approach would be to take the next order of mean field approximation (see (13)),

$$P_t(x_{i-1}, x_i, x_{i+1}) \approx \frac{P(x_{i-1}, x_i)P(x_i, x_{i+1})}{P(x_i)}. \quad (23)$$

This level of approximation leads to sets of nonlinear equations of up to fourth order on the parameters whose study, in the case of more than one parameter, belongs in the realm of algebraic surfaces and their intersections, an involved subject. We do not believe that such complications are worth pursuing given the simple-minded model of departure. Otherwise, the extension of the single-cell mean field approximation to two-dimensional models, with two or more states per cell, together with automated search for meaningful combinations of parameters may prove fruitful.

#### ACKNOWLEDGMENTS

The authors thank library specialist Angela K. Gruendl (UIUC) for providing a copy of reference [6]. JRGM acknowledges FAPESP, the São Paulo State Research Foundation, for partial support under research grant 2015/21580-0; YG acknowledges CAPES, the Coordenação de Aperfeiçoamento de Pessoal de Nível Superior, for a Ph. D. scholarship.

#### Appendix: Phase transitions in the mixed PCA of Table III

We mentioned in Sec. VI (see also Sec. V) that all PCA listed in Table III display an extinction-survival phase transition at some critical value of  $p$ . Here we give the critical

TABLE V. Critical points for the single-parameter mixed PCA listed in Table III at the single-cell mean field approximation ( $p_{\text{mf}}^*$ ) and from small scale numerical simulations ( $p_{\text{sim}}^*$ ). Uncertainties in the values of  $p_{\text{sim}}^*$  are approximately  $\pm 0.001$ .

Mixed PCA rule	$p_{\text{mf}}^*$	$p_{\text{sim}}^*$
$p222-q32$	1/3	0.543
$p182-q72$	1/3	0.563
$p54-q200$	1/3	0.576
$p150-q104$	1/3	0.573
$p22-q232$	1/3	0.589
$p146-q108$	0	0.648
$p18-q236$	0	0.676

points of the models obtained from the mean field equation (15) and also from small scale numerical simulations.

The critical point in the mean field approximation can be calculated as follows. In the stationary state  $x_{t+1} = x_t = x_\infty$ , and from (15) with  $a = 0$  we obtain that either  $x_\infty = 0$  or  $x_\infty$  is a solution of

$$(u - v + f)x_\infty^2 + (v - 2u)x_\infty + (u - 1) = 0, \quad (\text{A.1})$$

where  $u$ ,  $v$ , and  $f$  are the variables introduced in Subseq. IV A. The quadratic equation (A.1) has solutions

$$x_\infty^{(\pm)} = \frac{-(v - 2u) \pm \sqrt{(v - 2u)^2 - 4(u - v + f)(u - 1)}}{2(u - v + f)}. \quad (\text{A.2})$$

Now we must find the candidate critical points at which  $x_\infty^{(\pm)}(p) = 0$ . The candidate roots of (A.2) are easily seen to be the points at which  $4(u - v + f)(u - 1) = 0$ ; however, since  $u - v + f$  appears in the denominator of (A.2), the candidate roots are actually obtained from the condition  $u - 1 = 0$ . The critical point  $p_{\text{mf}}^*$  is then given by the root between 0 and 1 (if all solutions to  $u - 1 = 0$  is nonpositive,  $p_{\text{mf}}^* = 0$ ) and the mean field stationary density profile is the solution of (A.2) with  $x_\infty(p) \geq 0$  for  $p \geq p_{\text{mf}}^*$  (or, sometimes,  $p \leq p_{\text{mf}}^*$ ). The mean field critical points calculated for the mixed PCA of Table III are given in Table V, together with critical points  $p_{\text{sim}}^*$  estimated from numerical simulations of PCA of  $L = 8000$  cells with data obtained from 4000 samples of the stationary density for each value of  $p$  resolved in steps of  $\Delta p = 0.001$ .

With every continuous phase transition there comes the question of its universality class, i.e., of the critical exponents ruling the scaling behavior of the system at criticality [48, 49]. The determination of the critical behavior of PCA can be achieved by standard means—Monte Carlo simulations and finite-size scaling analysis [48, 49, 53, 54, 60]—, but is not our focus here. We guess, however, on the basis of the directed percolation conjecture [55, 56], according to which phase transitions into an absorbing state in short-ranged single component systems in the absence of conserved quantities all belong to the same universality class of critical behavior, that the critical behavior of the mixed PCA of Table III all belong to the directed percolation universality class.

- [1] J. von Neumann, *Theory of Self-Reproducing Automata*, W. A. Burks (ed.) (U. Illinois Press, Urbana and London, 1966).
- [2] S. Wolfram, Statistical mechanics of cellular automata, *Rev. Mod. Phys.* **55**, 601–644 (1983).
- [3] T. Toffoli, N. Margolus, *Cellular Automata Machines: A New Environment for Modeling* (MIT Press, Cambridge, MA, 1987).
- [4] B. Chopard, M. Droz, *Cellular Automata Modeling of Physical Systems* (Cambridge U. Press, Cambridge, UK, 1998).
- [5] A. Adamatzky, *Reaction-Diffusion Automata: Phenomenology, Localisations, Computation* (Springer, Berlin, 2013).
- [6] N. B. Vasil'ev, R. L. Dobrushin, I. I. Pyatetskii-Shapiro, Markov processes on an infinite product of discrete spaces, in: *Soviet-Japanese Symposium on Probability Theory*, Khabarovsk, USSR, August 1969, Proceedings (Akad. Nauk SSSR, Novosibirsk, 1969), Part 1, Vol. 2: Soviet Contributions, pp. 3–30 (in Russian).
- [7] N. B. Vasil'ev, M. B. Petrovskaya, I. I. Pyatetskii-Shapiro, Modelling of voting with random error, *Automat. Rem. Contr.* **30** (10), 1639 (1970).
- [8] N. B. Vasil'ev, I. I. Pyatetskii-Shapiro, The classification of one-dimensional homogeneous networks, *Probl. Inform. Transm.* **7** (4), 340 (1971).
- [9] O. N. Stavskaya, Gibbs invariant measures for Markov chains on finite lattices with local interaction, *Math. USSR Sb.* **21** (3), 395 (1973).
- [10] A. L. Toom, Nonergodic multidimensional system of automata, *Probl. Inform. Transm.* **10** (3), 239 (1978).
- [11] P. Gach, G. L. Kurdyumov, L. A. Levin, One-dimensional uniform arrays that wash out finite islands, *Probl. Inform. Transm.* **14** (3), 223 (1978).
- [12] A. L. Toom, N. B. Vasilyev, O. N. Stavskaya, L. G. Mityushin, G. L. Kurdyumov, S. A. Pirogov, Discrete local Markov systems, in: R. L. Dobrushin, V. I. Kryukov, A. L. Toom (eds.), *Stochastic Cellular Systems: Ergodicity, Memory, Morphogenesis* (Manchester U. Press, Manchester, 1990), pp. 1–182.
- [13] A. Georges, P. Le Doussal, From equilibrium spin models to probabilistic cellular automata, *J. Stat. Phys.* **54**, 1011 (1989).
- [14] J. L. Lebowitz, C. Maes, E. R. Speer, Statistical mechanics of probabilistic cellular automata, *J. Stat. Phys.* **59**, 117 (1990).
- [15] P. Hogeweg, Cellular automata as a paradigm for ecological modeling, *Appl. Math. Comput.* **27**, 81 (1988).
- [16] J. Silvertown, S. Holtier, J. Johnson, P. Dale, Cellular automaton models of interspecific competition for space—the effect of pattern on process, *J. Ecol.* **80**, 527 (1992).
- [17] G. B. Ermentrout, L. Edelstein-Keshet, Cellular automata approaches to biological modeling, *J. Theor. Biol.* **160**, 97 (1993).
- [18] R. Durrett, S. A. Levin, Stochastic spatial models: A user's guide to ecological applications, *Phil. Trans. R. Soc. London B* **343**, 329 (1994).
- [19] B. S. Soares-Filho, G. C. Cerqueira, C. L. Pennachin, DINAMICA – A stochastic cellular automata model designed to simulate the landscape dynamics in an Amazonian colonization frontier, *Ecol. Model.* **154**, 217 (2002).
- [20] D. G. Green, S. Sadedin, Interactions matter-complexity in landscapes and ecosystems, *Ecol. Complex.* **2**, 117 (2005).
- [21] S. F. Railsback, V. Grimm, *Agent-Based and Individual-Based Modeling: A Practical Introduction* (Princeton U. Press, Princeton, 2011).
- [22] M. J. Simpson, A. Merrifield, K. A. Landman, B. D. Hughes, Simulating invasion with cellular automata: Connecting cell-scale and population-scale properties, *Phys. Rev. E* **76**, 021918 (2007).
- [23] S. T. Johnston, R. E. Baker, D. L. Sean McElwain, M. J. Simpson, Co-operation, competition and crowding: A discrete framework linking Allee kinetics, nonlinear diffusion, shocks and sharp-fronted travelling waves, *Sci. Rep.* **7**, 42134 (2017).
- [24] F. Bagnoli, R. Rechtman, Stochastic bifurcations in the nonlinear parallel Ising model, *Phys. Rev. E* **94**, 052111 (2016).
- [25] L. Edelstein-Keshet, *Mathematical Models in Biology* (SIAM, Philadelphia, 2005).
- [26] F. Brauer, C. Castillo-Chavez, *Mathematical Models in Population Biology and Epidemiology*, 2nd ed. (Springer, New York, 2012).
- [27] A. Tsoularis, J. Wallace, Analysis of logistic growth models, *Math. Biosci.* **179**, 21 (2002).
- [28] R. M. May, Biological populations with nonoverlapping generations: stable points, stable cycles, and chaos, *Science* **186**, 645 (1974).
- [29] M. P. Hassell, J. H. Lawton, R. M. May, Patterns of dynamical behaviour in single-species populations, *J. Anim. Ecol.* **45**, 471 (1976).
- [30] R. May, Simple mathematical models with very complicated dynamics, *Nature* **261**, 459 (1976).
- [31] R. M. May, G. F. Oster, Bifurcations and dynamic complexity in simple ecological models, *Am. Nat.* **110**, 573 (1976).
- [32] P. Collet, J.-P. Eckmann, *Iterated Maps on the Interval as Dynamical Systems* (Birkhäuser, Boston, 1980).
- [33] R. L. Devaney, *An Introduction to Chaotic Dynamical Systems*, 2nd ed. (Addison-Wesley, Redwood, 1989).
- [34] W. C. Allee, *Animal Aggregations – A Study in General Sociology* (University of Chicago Press, Chicago, 1931).
- [35] B. Dennis, Allee effects: population growth, critical density and the chance of extinction, *Nat. Res. Model.* **3**, 481 (1989).
- [36] R. Lande, Demographic stochasticity and Allee effect on a scale with isotropic noise, *Oikos* **83**, 353 (1998).
- [37] P. A. Stephens, W. J. Sutherland, R. P. Freckleton, What is the Allee effect?, *Oikos* **87**, 185 (1999).
- [38] F. Courchamp, L. Berec, J. Gascoigne, *Allee Effects in Ecology and Conservation* (Oxford U. Press, Oxford, 2008).
- [39] A. M. Kramer, B. Dennis, A. M. Liebhold, J. M. Drake, The evidence for Allee effects, *Popul. Ecol.* **51**, 341 (2009).
- [40] K. S. Korolev, J. B. Xavier, J. Gore, Turning ecology and evolution against cancer, *Nat. Rev. Cancer* **14**, 371 (2014).
- [41] D. S. Boukal, L. Berec, Single-species models of the Allee effect: Extinction boundaries, sex ratios and mate encounters, *J. Theor. Biol.* **218**, 375 (2002).
- [42] M. A. Lewis, P. Kareiva, Allee dynamics and the spread of invading organisms, *Theor. Popul. Biol.* **43**, 141 (1993).
- [43] C. M. Taylor, A. Hastings, Allee effects in biological invasions, *Ecol. Lett.* **8**, 783 (2005).
- [44] Y. Gruntfest, R. Arditi, Y. Dombrovsky, A fragmented population in a varying environment, *J. Theor. Biol.* **185**, 539 (1997).
- [45] F. Courchamp, T. Clutton-Brock, B. Grenfell, Inverse density dependence and the Allee effect, *Trends Ecol. Evol.* **14**, 405 (1999).
- [46] H. A. Gutowitz, J. D. Victor, B. W. Knight, Local structure theory for cellular automata, *Physica D* **28**, 18 (1987).
- [47] D. ben-Avraham, J. Kohler, Mean-field  $(n, m)$ -cluster approximation for lattice models, *Phys. Rev. A* **45**, 8358 (1992).
- [48] J. Marro, R. Dickman, *Nonequilibrium Phase Transitions in Lattice Models* (Cambridge U. Press, Cambridge, UK, 1999).
- [49] H. Hinrichsen, Non-equilibrium critical phenomena and phase

- transitions into absorbing states, *Adv. Phys.* **49**, 815 (2000).
- [50] F. Bagnoli, R. Rechtman, Phase transitions of cellular automata, arXiv:1409.4284 [cond-mat.stat-mech] (2014).
  - [51] H. Fukś, N. Fatès, Local structure approximation as a predictor of second-order phase transitions in asynchronous cellular automata, *Nat. Comput.* **14**, 507 (2015).
  - [52] E. Domany, W. Kinzel, Equivalence of cellular automata to Ising models and directed percolation, *Phys. Rev. Lett.* **53**, 311 (1984).
  - [53] J. R. G. Mendonça, M. J. de Oliveira, An extinction-survival-type phase transition in the probabilistic cellular automaton  $p182-q200$ , *J. Phys. A: Math. Theor.* **44**, 155001 (2011).
  - [54] J. R. G. Mendonça, The inactive-active phase transition in the noisy additive (exclusive-or) probabilistic cellular automaton, *Int. J. Mod. Phys. C* **27**, 1650016 (2016).
  - [55] H. K. Janssen, On the nonequilibrium phase transition in reaction-diffusion systems with an absorbing stationary state, *Z. Phys. B* **42**, 151 (1981).
  - [56] P. Grassberger, On phase transitions in Schlögl's second model, *Z. Phys. B* **47**, 365 (1982).
  - [57] R. M. May, Bifurcations and dynamic complexity in ecological systems, *Ann. N. Y. Acad. Sci.* **316**, 517 (1979).
  - [58] T. D. Rogers, D. C. Whitley, Chaos in the cubic mapping, *Math. Model.* **4**, 9 (1983).
  - [59] R. M. May, Chaos and the dynamics of biological populations, *Nucl. Phys. B (Proc. Suppl.)* **2**, 225 (1987).
  - [60] J. R. G. Mendonça, Monte Carlo investigation of the critical behavior of Stavskaya's probabilistic cellular automaton, *Phys. Rev. E* **83**, 012102 (2011).